NASA Technical Memorandum 87213

Cyclic Creep Analysis from Elastic Finite-Element Solutions

A. Kaufman
Lewis Research Center
Cleveland, Ohio

and

S.Y. Hwang
South Carolina State College
Orangeburg, South Carolina

Prepared for the
1986 Southeastern Conference on Theoretical and Applied Mechanics
sponsored by the University of South Carolina
Columbia, South Carolina, April 17-18, 1986

NASA

CYCLIC CREEP ANALYSIS FROM ELASTIC FINITE-ELEMENT SOLUTIONS

A. Kaufman
National Aeronautics and Space Administration
Lewis Research Center
Cleveland, Ohio 44135

and

S.Y. Hwang
South Carolina State College
Orangeburg, South Carolina

SUMMARY

A uniaxial approach was developed for calculating cyclic creep and stress relaxation at the critical location of a structure subjected to cyclic thermomechanical loading. This approach was incorporated into a simplified analytical procedure for predicting the stress-strain history at a crack initiation site for life prediction purposes. An elastic finite-element solution for the problem was used as input for the simplified procedure. The creep analysis includes a self-adaptive time incrementing scheme. Cumulative creep is the sum of the initial creep, the recovery from stress relaxation and the incremental creep. The simplified analysis was exercised for four cases involving a benchmark notched plate problem. Comparisons were made with elastic-plastic-creep solutions for these cases using the MARC nonlinear finite-element computer code.

E-2872

INTRODUCTION

This paper discusses the development of a uniaxial creep procedure for computing cyclic creep and stress relaxation at the critical location in a structure. While nonlinear, three-dimensional, finite-element computer codes are available for calculating cyclic stress-strain response, these are frequently too costly in computing time and other resources to be practical in the early design stages for complex structures. Computing costs in particular, limit three-dimensional, nonlinear finite-element analyses to a small number of cycles which may not be sufficient for life prediction purposes in cases involving creep ratchetting. The NASA Lewis Research Center has been sponsoring contractual and inhouse efforts to develop simplified methods for predicting the stress-strain history at a crack initiation site (ref. 1) as part of its life improvement programs for hot gas path components in aircraft engines and space power vehicles. This study was undertaken to improve the creep analysis capability of an in-house developed simplified inelastic analysis procedure. This procedure (refs. 2 to 3) performs a uniaxial nonlinear analysis for the critical location in a structure based on elastic solutions from three-dimensional finite-element analyses.

The underlying assumption of this simplified procedure is that the inelastic regions are localized and constrained by the bulk of the surrounding elastic material. Therefore, the total strain history calculated from three-dimensional, elastic finite-element analyses for various points in the mission

cycle can be used as input in elastic-plastic analyses for cyclic thermal loading. The elastic strain cycle is divided into a sufficient number of load-time steps to realistically determine the cyclic stress-strain hysteresis loops from inelastic analyses. Neuber-type corrections (ref. 4), including corrections for residual stresses, can be incorporated into the plasticity computations to account for strain redistribution during mechanical loading cycles (ref. 5). This analytical procedure, with appropriate constitutive models to define the material cyclic behavior, was automated in a computer code. Since the simplified procedure is uniaxial, the input and output is based on von Mises effective stresses and strains. Signs have to be assigned to the input effective strains from the elastic analyses by the user, usually on the basis of the sign of the dominant principal strain. A kinematic hardening model was used to determine cyclic yielding for the problems discussed herein.

A power law type of creep constitutive equation was assumed to represent primary stage creep. This was used in conjunction with a time hardening rule for relating creep strain change to stress change. There is also provision in the computer code for a modified strain hardening rule where the primary creep is reinitiated and reversed with each reversal of the creep straining direction. The uniaxiality of the simplified procedure requires that the user exercise judgement in directing the form of the creep analysis. Three options are available in the code: (1) stress relaxation at constant strain, (2) cumulative creep at constant stress or (3) a combination of stress relaxation and creep accumulation. This last option is the one of interest for most practical problems involving high-temperature creep. Previously, the combined stress relaxation and creep strain change was obtained by averaging the results for the first two options for each specified time step.

The purpose of this study was to develop a more rational and accurate creep analysis approach for combined creep and stress relaxation for inclusion in the simplified analysis procedure. The approach that was developed included a self-adaptive time incrementing scheme for subdividing the specified dwell times into increments. At the start of the creep computations for each dwell time, the time period of the initial increment was automatically determined from preset tolerances on the permitted stress and incremental creep strain changes. Creep for any subsequent increment was calculated using a time period that was a constant multiple of the previous time period. In this approach, the cummulative creep strain at the end of the time period is the sum of the creep at the beginning of the time period, the creep recovery from stress relaxation and the incremental creep strain during the time period. The creep recovery component is obtained by first calculating the stress relaxation for each increment on the basis of constant strain boundary conditions, then assuming some proportionate recovery of the stress relaxation and calculating the creep strain change required for this recovery. For the initial increment, the creep recovery portion of the stress is assumed to be two thirds of the stress relaxation. For each subsequent increment, the percent of creep recovery increases by a fixed amount until full recovery is attained. These assumptions were derived from experience in conducting a large number of nonlinear finite-element analyses of elastic-plastic-creep problems.

The improved simplified creep analysis was incorporated into the previously developed computer code. Input consists of inelastic material properties in the form of coefficients and exponents for elastic-plastic and creep constitutive equations, dwell times at precribed points during the cycle and

the total strain history at the critical location from elastic finite-element analyses. Four cases involving a benchmark notched plate problem (ref. 6) subjected to cyclic mechanical loading were analytically examined to verify the accuracy of the simplified creep analysis approach. The first two cases had maximum creep strains of about 0.2 percent during the tensile or loading part of the cycle and the third case had a maximum creep strain under 0.1 percent during the compressive unloading part of the cycle. The fourth case involved a combination of both tensile and compressive creep as an illustration of a cyclic creep problem. Elastic and nonlinear finite element analyses were performed for all four cases using the MARC computer code. The elastic solutions for the notch root location were used as input for the simplified analysis computer code. Comparisons between the simplified and MARC nonlinear finite-element analyses of these cases were made with particular attention to the creep portions of the stress-strain histories at the critical location.

The comparisons demonstrated that the uniaxial creep analysis method can duplicate the creep strains in the cyclic stress-strain hysteresis loops computed from the nonlinear, three-dimensional, finite-element analyses to a high degree of accuracy and have greater computational stability than the latter. For the benchmark problems, the simplified procedure used less than 1 percent of the central processor (CPU) time required by the MARC cyclic analyses.

SYMBOL LIST

A,B,C	temperature-dependent constants in creep power law, equation (1)
E	modulus of elasticity
E_e	modified modulus of elasticity, $3E/(2(1+\mu))$
E_p	work hardening slope (fig. 3)
K,n	temperature-dependent constants in cyclic stress-strain law, equation (13)
r	time multiple constant
t	creep time
t_i	creep time at beginning of ith time increment
α	effective stress change tolerance coefficient
γ_i	time scale coefficient for ith time increment
$\Delta\varepsilon_{ci}$	equivalent creep strain change at ith time increment
Δt_i	ith time increment
ε	equivalent total strain

ε_c equivalent creep strain

ε_{ci} equivalent creep strain at beginning of ith time increment

ε_{cRi} equivalent creep recovery strain at beginning of ith time increment

ε_p equivalent plastic strain

ε_p' maximum equivalent plastic strain in cycle (fig. 3)

θ_i percent creep recovery for ith time increment

μ Poisson's coefficient

σ effective stress

σ' maximum effective stress in cycle (fig. 3)

σ_i effective stress at beginning of ith time increment

σ_{yi} initial yield stress in loading part of cycle

σ_{yi}' initial yield stress in unloading part of cycle

ANALYTICAL PROCEDURE

A simplified cyclic creep procedure was developed for computing cyclic creep and stress relaxation at the critical crack initiation critical location in a structure. In this approach, a power law type of creep constitutive equation was assumed to represent uniaxial primary creep behavior.

$$\varepsilon_c = \left(\frac{\sigma}{A}\right)^{B_t C} \tag{1}$$

A typical stress-strain cycle with creep dwell times at the maximum and minimum total strain parts of the cycle is illustrated in figure 1. A modified time-hardening law, as shown in figure 2, was proposed to determine the stress change at the ith time increment during a dwell time in the cycle. The equation, which is derived in Appendix A, takes the form

$$\sigma_{i+1} = \left\{ (1 - \theta_i) \left[\frac{1}{1 + (1 + \gamma_i) \frac{\Delta t_i}{t_i}} \right]^C (\sigma_{i-1}^B - \sigma_i^B) + \left[\frac{1}{1 + \gamma_i \, \Delta t / t_{i+1}} \right]^C \sigma_i^B \right\}^{1/B}, \qquad i = 1 \ldots n \qquad (2)$$

where γ_i, the time scale coefficient, was assumed to increase proportionately between the two limiting values (γ_1 and γ_∞). These values were computed from the following expression

$$\gamma_i = \left[\frac{1}{(1 - \alpha)^{B/C}} - 1 \right] \left[\frac{1}{r^{i+1}} \sum_{n=1}^{i} r^n \right] \qquad (3)$$

In equation (3), α is the tolerance on the allowable stress change per increment and r is a constant relating the current time increment to the preceding one. The latter is defined as

$$r = \frac{\Delta t_{i+1}}{\Delta t_i} \qquad (4)$$

The value of r is assumed to be 1.5, the same ratio used in MARC automatic creep computations. It follows that

$$\Delta t_{i+1} = 1.5 \, \Delta t_i \qquad (5)$$

and

$$t_{i+1} = t_i + \Delta t_i$$

Equation (3) yields two limiting values:

$$\gamma_1 = \frac{2}{3} \left[\frac{1}{(1 - \alpha)^{B/C}} - 1 \right]$$

when $i = 1$

and

$$\gamma_\infty = 2\left[\frac{1}{(1-\alpha)^{B/C}} - 1\right] \tag{6}$$

as $i \to \infty$

To better fit data points with those obtained from MARC creep analyses, instead of using equation (3) for γ_i, γ_i was determined by a constant multiple of 7/6 of γ_{i-1} until its value reached γ_∞. Then, for the remaining time increments γ_∞ will be used throughout.

In equation (2), θ_i denotes the percent of creep recovery at the i^{th} time increment. For the initial time period, the creep strain recovered is assumed to be two-thirds of the stress relaxation. For each subsequent increment, the percentage increases by a fixed amount until a full recovery is attained. Thus

$$\theta_i = \frac{2}{3} + \frac{i-1}{30}$$

$$i = 1 \ldots . n \tag{7}$$

Full recovery is assumed to have been attained at the tenth increment. The above assumptions were derived from experience in conducting a large number of nonlinear finite-element analyses of elastic-plastic-creep problems.

It should be noted that, in using equations (2) and (5) for each dwell time in a cycle, the initial time period, Δt_1, must be estimated first. A self-adaptive time-incrementing scheme (eq. (5)) was used to subdivide the remainder of the specified dwell time into a number of increments. At the start of the creep computation, the initial stress level, σ_1, was known from he calculated stress for the preceding increment. The initial time period, Δt_1, was estimated from the preset tolerances on the permissable stress and incremental creep strain changes, the initial stress level, the initial creep recovery, and the constants of the creep constitutive power law. The resulting equation takes the form

$$\Delta t_1 = \left[\frac{\Delta\varepsilon_c}{\left(\frac{1}{A}\right)^B \left\{(1-\alpha)^B\left[(1+r)^C + \theta_2 - 1\right] - \theta_2\sigma\right\}_1^B}\right]^{1/C} \tag{8}$$

where $\Delta\varepsilon_c$ is the change of the initial creep, which is assumed to be equal to the change of the corresponding elastic strains. Since the von Mises yield criterion was used, the total strain from a uniaxial stress-strain curve has to be converted into a modified equivalent total strain (ref. 8). This modified elastic part of the equivalent total strain corresponds to the measured elastic strain multiplied by $2(1+\mu)/3$. For computational convenience, this factor was included in a modified elastic modulus defined by $E_e = 3E/(2(1+\mu))$.

Using the relationship $(\sigma_1 - \sigma_2)/E_e$ for $\Delta\varepsilon_c$ and imposing the stress change tolerance, equation (8) is reduced to

$$\Delta t_1 = \left[\frac{\alpha}{E_e \left(\frac{1}{A}\right)^B (1-\alpha)^B \left\{ [(1+r)^C + \theta_2 - 1] - \theta_2 \right\} \sigma_1^{(B-1)}} \right]^{1/C} \tag{9}$$

With Δt_1, known from equation (9), the subsequent time increments follow equation (5). At the beginning of the dwell time; $i = 1$, $t_1 = 0$, $\varepsilon_{c1} = 0$ and Δt_1 was obtained from equation (9). At any other creep time, the cumulative creep strain up to t_{i+1} is the sum of the creep strain, ε_{ci}, at the beginning of time period t_i, the creep recovery, $\theta_i \varepsilon_{cRi}$, from stress relaxation, and the incremental creep strain, $\Delta\varepsilon_{ci}$. These relations can be expressed as

$$\varepsilon_{c(i+1)} = \varepsilon_{ci} + \Delta\varepsilon_{ci} - \theta_i \varepsilon_{cRi} \tag{10}$$

where

$$\Delta\varepsilon_{ci} = \left(\frac{1}{A}\right)^B \sigma_i^B \left(t_{i+1}^C - t_i^C\right) \tag{11}$$

and

$$\varepsilon_{cRi} = \left(\frac{1}{A}\right)^B \left(\sigma_{i-1}^B - \sigma_i^B\right) t_i^C \tag{12}$$

It should be noted that equation (12) is exact only if the fully relaxed stress under constant strain boundary conditions is used for σ_i rather than the partially recovered stress shown in figure 2. However, the difference between these two stress values is slight for the small tolerance normally held on the stress change. When full recovery is attained and $\theta_i = 1$, these stress values become identical. In view of these considerations and for the sake of simplicity, the partially recovered stress level σ_i shown in figure 2 may be accepted as the one to use in equation (2).

The computational scheme started at the known effective stress-equivalent strain at the beginning of creep. The initial time period was determined from equation (9) and the initial time scale γ_1 from equation (6). Subsequent time increments follow equation (5). With these quantities known from the above procedure, the stress level at the end of the initial time period can be obtained from equation (2) and the corresponding cumulative creep strains from equations (10) to (12). Subsequent stress relaxations and creep strain accumulations follow the same computational scheme. Sample calculated results for the first case analyzed are shown in table I.

The creep analysis approach described above was incorporated in the computer code previously developed to automate the simplified analytical procedure. This procedure initially follows the elastic effective stress-equivalent strain input until the occurrence of initial yielding. The stress-strain solution then proceeds along the initial yield surface as determined from the

stress-strain properties. At each load step during yielding the stress shift (difference between new yield stress and stress predicted from elastic analysis) from the original input data is calculated. Elastic load reversal is signaled when the input stress is less than the yield stress from the previous load step. During elastic unloading, the stresses are translated from the original elastic analysis solution by the amount of the calculated stress shift. Reverse yielding occurs when the stress reaches the reverse yield surface as determined from the hardening model. Again, the solution follows the yield surface until another load reversal is indicated when the stress based on the shifted elastic solution is less than the yield stress. The elastic response during load reversal is obtained by translating the original elastic solution according to the new stress shift calculated during reversed yielding. The stress-strain response for subsequent cycles is computed by repeating this procedure of identifying load reversals, tracking reverse yield surfaces and translating the original elastic solution during elastic loading and unloading. The creep computations previously discussed are performed for all load steps involving dwell times.

Neuber-type corrections for strain redistribution during mechanical loading cycles were implemented in the plasticity calculations. The strain redistribution correction is applied to the ideal local total strain obtained from the elastic solution. These corrections were incorporated in a version of the computer code using a kinematic hardening model to characterize the yield surface under cycling. A representation of a cyclic stress-strain curve by a bilinear kinematic hardening model is illustrated in figure 3. The loci of the tips of the cyclic curves is described by the relation

$$\sigma = K(\varepsilon_p)^n \tag{13}$$

The work hardening slope, E_p, for the kinematic hardening model was determined from energy considerations to give the same strain energy, as indicated by the enclosed area in figure 3, as the actual stress-strain curve. This work hardening slope is defined by

$$E_p = \frac{\sigma'}{\varepsilon_p'}\left(\frac{2n}{1+n}\right) \tag{14}$$

The code will automatically avoid these corrections for thermal loading problems where there are no applied mechanical loads. Without applied loads, the Neuber method would be inapplicable since the stress/strain concentration equations would have zero net stresses and strains in the denominators. Provision is also made for the user to circumvent the corrections for other situations where they would not be appropriate. These situations include locally strain controlled problems and problems where the total strain input is based on strain measurements rather than elastic finite-element analyses.

Since the stable cyclic stress-strain hysteresis loop is a function of the plastic strain range, it is necessary to iterate between the maximum plastic strain assumed for the stress-strain relation of equation (14) and the resulting calculated maximum plastic strain. This iterative process is continued until the specified and calculated maximum plastic strains are in

reasonable agreement, usually within three iterations. Each iteration causes some change in the size and shape of the cyclic stress-strain hysteresis loop. These changes, although usually small, make it difficult to directly compare solutions from the simplified procedure against nonlinear finite-element analyses since the cyclic stress-strain curves would be somewhat different.

The computer program was validated by conducting simplified analyses for the benchmark notch problem and comparing the results to those from MARC nonlinear analyses. The geometry of the benchmark notch specimen is illustrated in figure 4. This specimen was tested under isothermal conditions as part of a program to provide controlled strain data for constitutive model verification. The benchmark notch test was conducted by fully-reversed mechanical load cycling at a constant temperature of 649 °C. A MARC analysis of this problem using kinematic hardening demonstrated excellent agreement with experimental data (ref. 9). Unfortunately, the dwell times in the cyclic tests were too short to achieve significant creep strains. Therefore, nonexperimental cases involving longer dwell times at the peak strain levels were devised to evaluate the simplified creep analysis method. Four variations of the benchmark notch problem were analyzed; two with maximum creep strains of about 0.2 percent on the tensile or loading part of the cycle, a third with a maximum creep strain under 0.1 percent on the compressive or unloading part of the cycle and a fourth case involving combined tensile and compressive creep to illustrate a cyclic creep problem. Cyclic yielding was described by a kinematic hardening model with cyclic stress-strain data for Inconel 718 alloy (ref. 6). Nonlinear and elastic MARC analyses of this problem were performed using approximately 600 triangular plane strain elements to model a quarter segment bounded by planes of symmetry as shown in figure 5. The MARC solutions shown for the benchmark notch specimen were computed at the closest Gaussian integration point to the root of the notch.

DISCUSSION OF ANALYTICAL RESULTS

Analytical results for the benchmark notch cases using the improved creep analysis incorporated in the simplified inelastic procedure are discussed herein. Comparisons are made with MARC finite-element solutions for the same problems. Stress-strain cycles used for comparison purposes are in terms of von Mises effective stresses and equivalent strains with assigned tensile or compressive signs. The entire discussion is based on the critical location, which was at the notch root.

The conditions of the four analytical cases studied are summarized in table II. The analyses for the first three cases were conducted by enforcing the same initial stress at the start of creep on the simplified procedure as was calculated for the comparable MARC analysis. This was necessary because small differences in the cyclic stress-strain curves could cause differences in the initial stresses of about 3 percent and make it difficult to directly compare both creep analysis methods.

In cases 1 and 2, 4-hr dwell times were imposed at the maximum tensile load, or the maximum total strain part of the cycle. These two cases differ

in the load level at the start of creep. In both cases the MARC finite-element analyses broke down after reaching a creep microstrain of 1000 (or less than 1 hr of accumulated creep time) because of inability to maintain the relatively tight tolerance on the stress change per increment. Opening up the tolerance by an order of magnitude enabled the finite-element creep computations to be extended to 1.5 hr of accumulated dwell time. However, the looser tolerance resulted in a more erratic calculated stress relaxation response until the finite-element creep analysis was automatically terminated due to instability. In contrast, the simplified analysis exhibited no computational problems and gave a stable solution for the full 4-hr dwell times. Comparison of the simplified creep analyses with the MARC analyses, as far as they could be carried out, are shown in figures 6 (a) and (b) for cases 1 and 2 respectively. Excellent agreement is seen between the two analytical methods for both cases.

In case 3, a 4-hr dwell time was applied at the minimum load in the cycle. Since the stress level at the start of creep was much smaller than in the first two cases, there was no computational problem with the finite-element creep analysis for case 3. Again, excellent agreement was shown between the simplified and finite-element creep analyses as is demonstrated in figure 6(c). In all three cases, the simplified solution agreed with the finite element results within 1 percent in terms of stress during relaxation and 6 percent in terms of creep strain.

The ability of the simplified method to calculate cyclic creep was evaluated in case 4. Dwell times were applied at both the maximum and minimum cyclic load levels. The dwell time at the maximum load was limited to 1 hr to avoid the computational instability problem with the finite element analysis at longer dwell times. A 10-hr dwell time, rather than 4 hr as in case 3, was applied at the minimum load to obtain larger creep strains in the minimum strain part of the cycle. A comparison of the simplified and finite-element solutions for case 4 is shown in figure 7. The comparison was limited to the first cycle because of the difficulty of maintaining computational stability during the second cycle for the finite element analysis. Calculated points from the simplified analysis are shown only for the beginning and end of each dwell time. There is a noticeable difference between the creep behavior during the compressive dwell time shown in figure 7 and that illustrated in figure 1. This difference is due to the fact that Since the finite-element analysis considers the equivalent creep strain change during compression as a positive number, the magnitude of the total strain during the second dwell period can only be reduced. To maintain consistency with the MARC creep analysis, the simplified analysis was adapted to have the same type of creep behavior on load reversal. However, for an actual structural analysis of a cyclic creep problem the simplified procedure would consider a creep strain change during compression as a negative number and give the behavior shown during the compressive dwell time in figure 1.

Most of the discrepancies between the simplified and finite-element hysteresis loops in figure 7 were due primarily to the iteration process built into the simplified analysis computer code which resulted in the use of a cyclic stress-strain curve slightly different from that used in the MARC elastic-plastic analysis. During the initial monotonic loading, the two analytical methods agreed, as in cases 1 to 3, within 1 percent in relaxed

stress and 6 percent in creep strain. However, during load reversal dwell time the differences increased to 1.8 percent in terms of relaxed stress and almost 2 to 1 in terms of cumulative creep strain. The larger disagreement in creep strain was mainly due to the accumulation of error as one proceeds through the cycle and the sensitivity of creep calculations to relatively small discrepancies in the stress levels. The simplified analysis of the benchmark notch problem for case 4 used 0.3 percent of the central processor unit (CPU) time required for the MARC nonlinear analysis of the finite element model shown in figure 5. The MARC computing time could have been reduced by concentrating on the notch region and applying proper boundary conditions. However, the simplified procedure would still be much faster because it focusses on a single point.

SUMMARY OF RESULTS

An improved uniaxial creep analysis method was developed for use with a simplified inelastic analysis procedure for calculating the stress-strain history at the critical location of a thermomechanically cycled structure. This creep method used a self-adaptive time incrementing scheme for subdividing the dwell time period into smaller increments for creep analysis. In this approach, cumulative creep was the sum of the initial creep strain, the recovery from stress relaxation and the incremental creep strain. Neuber-type corrections were applied to account for strain redistribution and residual stresses due to plastic strain reversals. Analytical predictions from the simplified procedure for benchmark notched plate problems were compared to nonlinear finite-element solutions. The following general conclusions were drawn from the evaluation
of the method:

1. The predicted stress-strain response using the simplified procedure with the uniaxial creep analysis showed excellent agreement with three-dimensional elastic-plastic-creep finite element solutions using the MARC program. In all the monotonic creep analysis cases studied, the simplified and finite-element solution for the critical crack initiation location agreed within one percent in terms of relaxed stress and 6 percent in terms of cumulative creep strain.

2. The simplified creep analysis was extremely stable. Creep calculations could be carried out to tight tolerances on stress changes and continued under conditions where the nonlinear finite-element analysis became computationally unstable and broke down.

3. The simplified procedure computed stress-strain hysteresis loops for the critical location using 0.3 percent of the CPU time required for elastic-plastic-creep finite-element analyses of the full finite element model.

APPENDIX A
DERIVATION OF BASIC CREEP EQUATIONS

Equation (2) is obtained by combining equations (1), (10), (11) and (12). From equation(10)

$$\varepsilon_{c(i+1)} = \varepsilon_{ci} + \Delta\varepsilon_{ci} - \theta_i \varepsilon_{cRi}$$

Substituting equation (1) for ε_{ci}, equation (11) for $\Delta\varepsilon_{ci}$ and equation (12) for ε_{cRi} yields

$$\varepsilon_{c(i+1)} = \left(\frac{1}{A}\right)^B \sigma_{i-1}^B \, t_i^C + \left(\frac{1}{A}\right)^B \sigma_i^B (t_{i+1}^C - t_i^C) - \left(\frac{1}{A}\right)^B \theta_i (\sigma_{i-1}^B - \sigma_i^B) t_i^C$$

or

$$\varepsilon_{c(i+1)} = \left(\frac{1}{A}\right)^B \left\{(1 - \theta_i)[\sigma_{i-1}^B - \sigma_i^B] t_i^C + \sigma_i^B \, t_{i+1}^C\right\}$$

From figure 2, the creep strain at the end of an increment is given by

$$\varepsilon_{c(i+1)} = \left(\frac{1}{A}\right)^B \sigma_{i+1}^B \, [t_{i+1} + \gamma_i \, \Delta t_i]^C + \left(\frac{1}{A}\right)^B \sigma_{i+1}^B \, [t_i + (1 + \gamma_i) \, \Delta t_i]^C$$

Equating the above two expressions leads to the form of equation (2)

$$\sigma_{i+1} = \left\{(1 - \theta_i) \left[\frac{1}{1 + (1 + \gamma_i) \dfrac{\Delta t_i}{t_i}}\right]^C (\sigma_{i-1}^B - \sigma_i^B) + \left[\frac{1}{1 + \gamma_1 \, \Delta t_i / t_{i+1}}\right]^C \sigma_i^B \right\}^{1/B}$$

Other equations given in the Analytical Procedure can be obtained from similar mathematical manipulations.

REFERENCES

1. Kaufman, A.; and Moreno, V.: Two Simplified Procedures for Predicting Cyclic Material Response from a Strain History. Nonlinear Constitutive Relations for High-Temperature Applications-1984. NASA CP-2369, 1985, pp. 201-219.

2. Kaufman, A.: Development of a Simplified Procedure for Cyclic Structural Analysis. NASA TP-2243, 1984.

3. Kaufman, A.: A Simplified Method for Elastic-Plastic-Creep Structural Analysis. J. Eng. Gas Turbines Power, vol. 107, no. 1, Jan. 1985, pp. 231-237.

4. Neuber, H.: Theory of Stress Concentration for Shear-Strained Prismatical Bodies with Arbitrary Nonlinear Stress-Strain Law. J. Appl. Mech., vol. 28, no. 4, Dec. 1961., pp. 544-550.

5. Kaufman, A.; and Hwang, S.Y.: Local Strain Redistribution Corrections for a Simplified Inelastic Analysis Based on an Elastic Finite-element Analysis. NASA TP-2421, 1985.

6. Domas, P.A.; et al.: Benchmark Notch Test for Life Prediction. NASA CR-165571, 1982.

7. MARC General Purpose Finite Element Program. Vol. A: User Information Manual; Vol. B: MARC Element Library. MARC Analysis Research Corporation, 1980.

8. Mendelson, A.: PLASTICITY: Theory and Application. MacMillan, New York, 1968.

9. Kaufman A.: Evaluation of Inelastic Constitutive Models for Nonlinear Structural Analysis. Nonlinear Constitutive Relations for High Temperature Applications, NASA CP-2271, 1983, pp. 89-106.

TABLE I. - SAMPLE CALCULATION (CASE 1)

Inc	t_i, hr	Δt_i, hr	t_{i+1}, hr	$\Delta\varepsilon_{ci}$	θ_i	ε_{cRi}	ε_{ci}, $\times 10^4$	Total equivalent strain, $\varepsilon_{c(i+1)}$		Effective stress, σ_{i+1}, MPa	
								Simplified	MARC	Simplified	MARC
1	0	0.002767	0.002767	1.385×10^{-4}	0	0	0	1.385×10^{-4}	1.402x10-4	809.7	809.0
2	0.002767	.002767	.005535	.478	0.0444	1.385	1.818	1.793		807.8	810.1
3	.005535	.004151	.009686	.501	.0213	1.818	2.298	2.323		806.1	807.1
4	.009686	.006226	.01591	.554	.0253	2.298	2.827	2.826		804.1	804.5
5	.01591	.00934	.02525	.6262	.0358	2.827	3.417	3.396		802.0	801.7
6	.02525	.01401	.03926	.7201	.0430	3.417	4.086	4.031		799.4	798.7
7	.03926	.02101	.06028	.8292	.0745	4.086	4.841	4.751		796.4	795.4
8	.06028	.03152	.09180	.9581	.1464	4.841	5.652	5.565		792.3	791.9
9	.09180	.04728	.1391	1.098	.1917	5.652	6.566	6.490		787.4	788.1
10	.1391	.0709	.2100	1.246	.256	6.566	7.555	7.536		783.6	784.0
11	.2100	.1064	.3164	1.447	.243	7.555	8.759	8.723		779.7	779.7
12	.3164	.1596	.4760	1.669	.301	8.759	10.127	10.060		775.5	775.2
13	.4760	.2394	.7153	1.926	.361	10.127	11.692	11.580		771.4	770.6
14	.7153	.3591	1.0744	2.199	.541	11.692	13.352			766.1	770.6
15	1.0744	.5387	1.6131	2.527	.532	13.352	15.347			761.7	
16	1.6131	.8081	2.4212	2.905	.625	15.347	17.627			757.1	
17	2.4212	1.2122	3.6334	3.334	.734	17.627	20.228			752.5	
18	3.6334	.3666	4.0000	.845	.746	20.228	20.327			752.1	

Δt_1 = 0.05 hr
t = 4 hr
α = 0.01

TABLE II. - ANALYTICAL CASES

Case	Load applied during dwell time, kN	Dwell time, hr	Tolerance coefficient on stress change	
			Simplified analysis	MARC analysis
1	33.3	4	0.01	0.01
2	35.1	4	.01	.01
3	-17.3	4	.01	.01
4	35.1	1	.01	.10
	-17.3	10	.01	.10

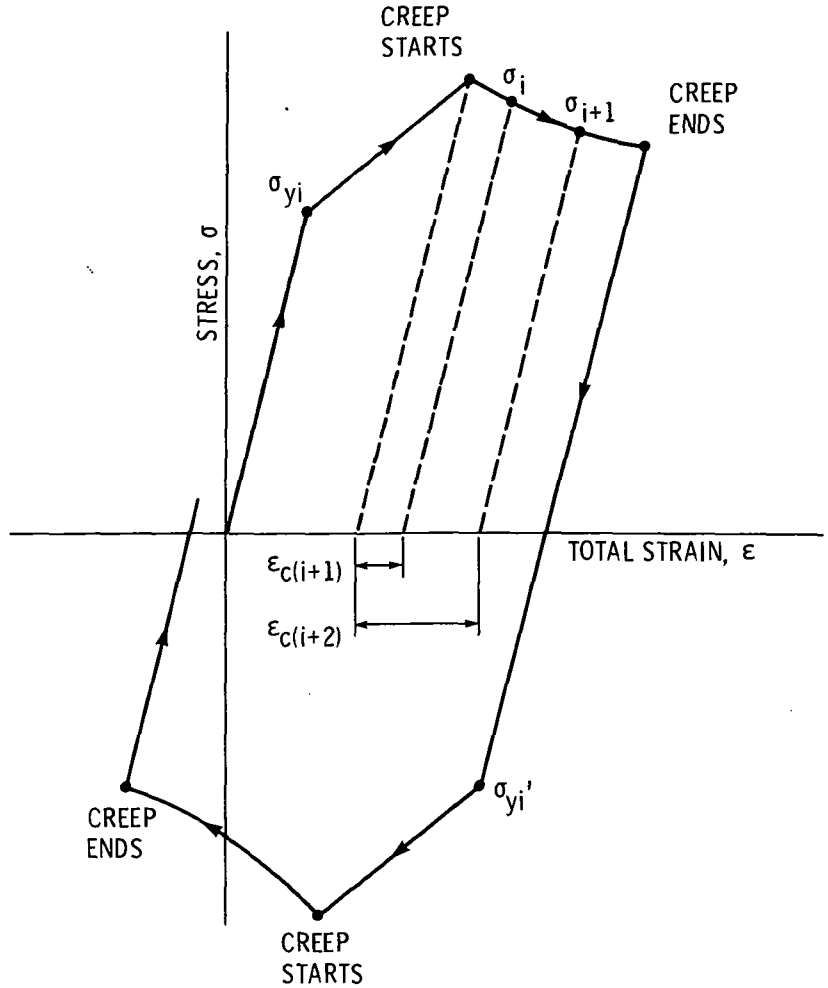

Figure 1. - Typical stress-strain cycle with creep dwell times.

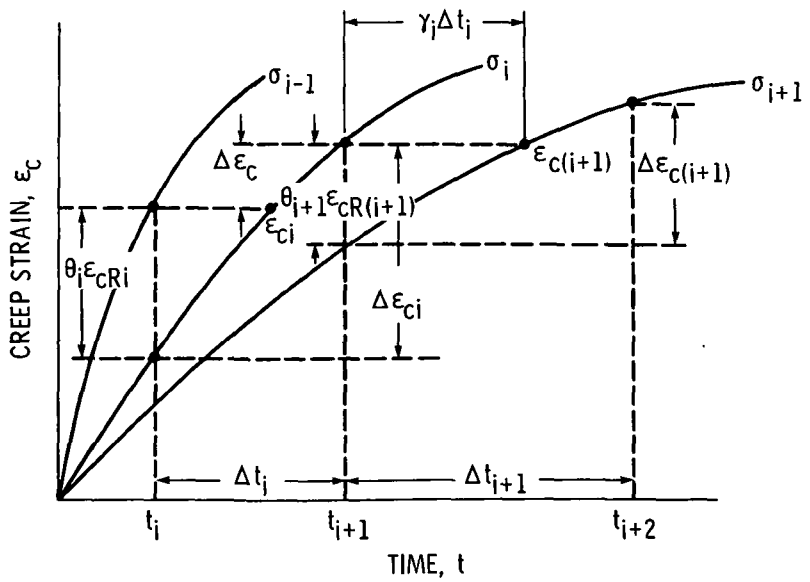

Figure 2. - Modified time hardening law.

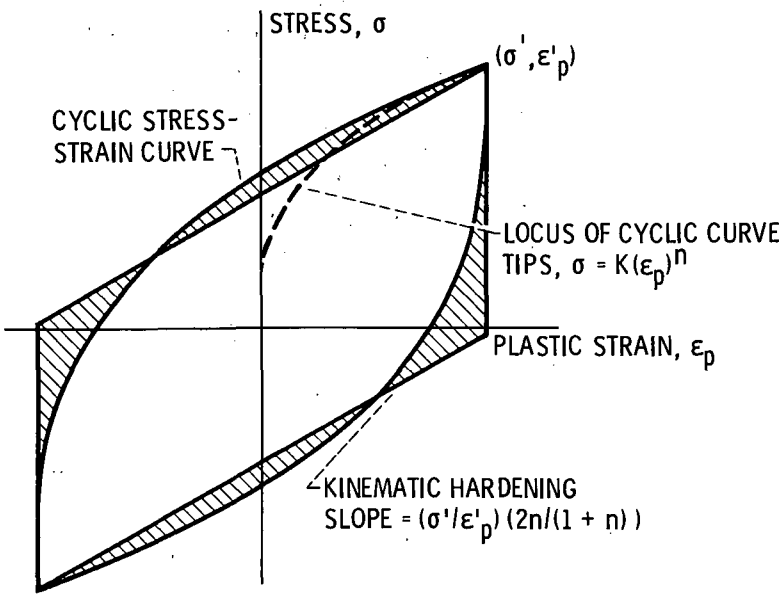

Figure 3. - Cyclic stress-strain representation.

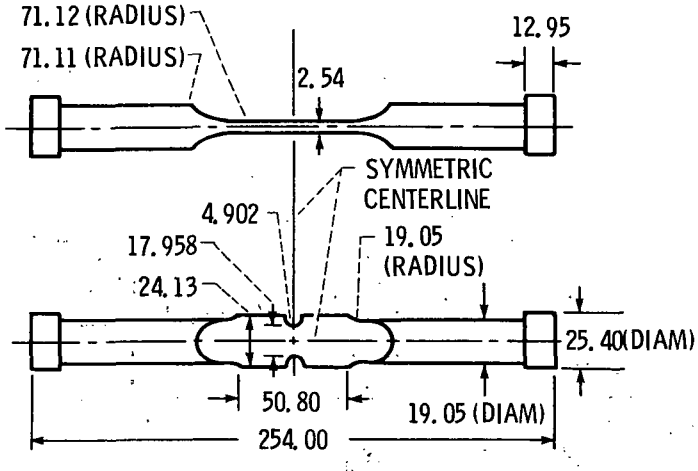

Figure 4. - Benchmark notch specimen (K_t = 1.9). (All dimensions in mm.)

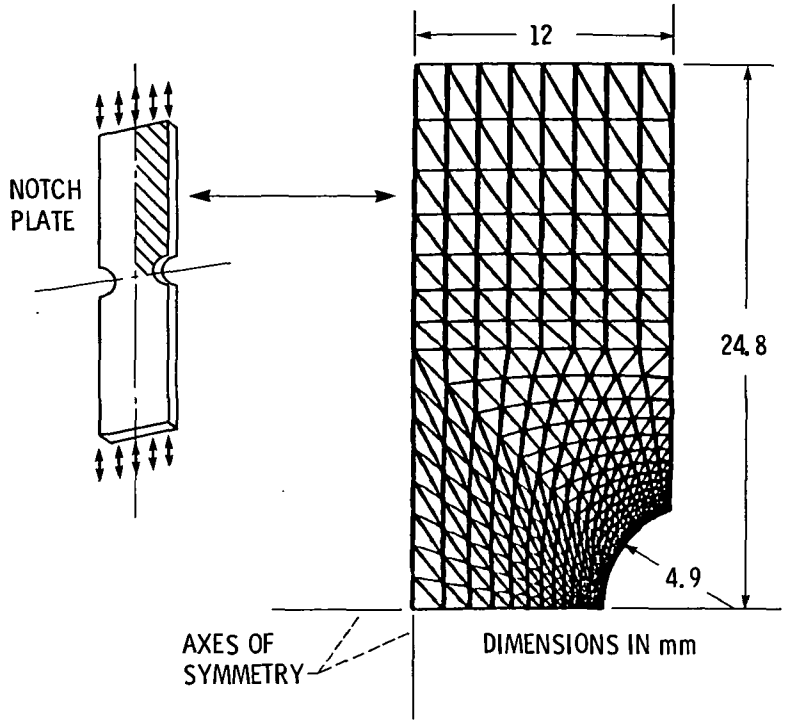

Figure 5. - Benchmark specimen finite-element model.

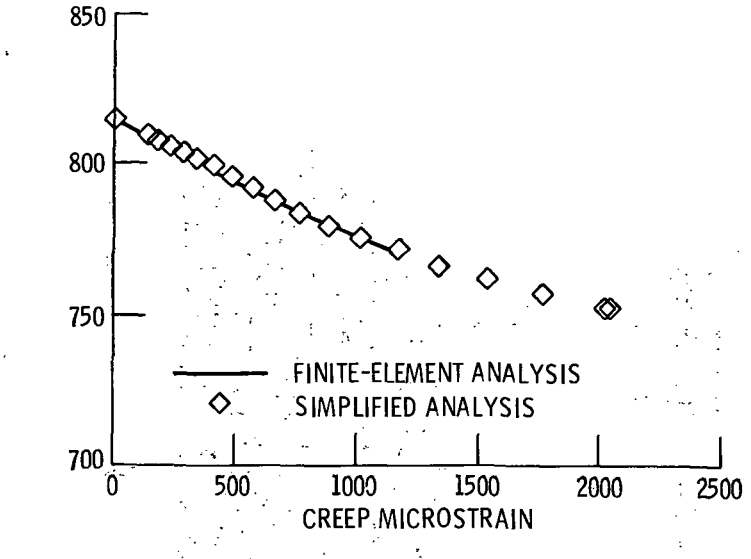

(a) Case 1.

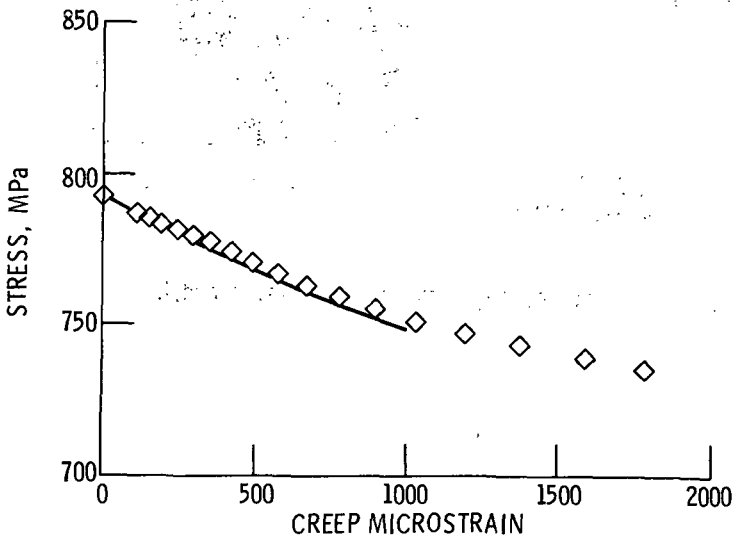

(b) Case 2.

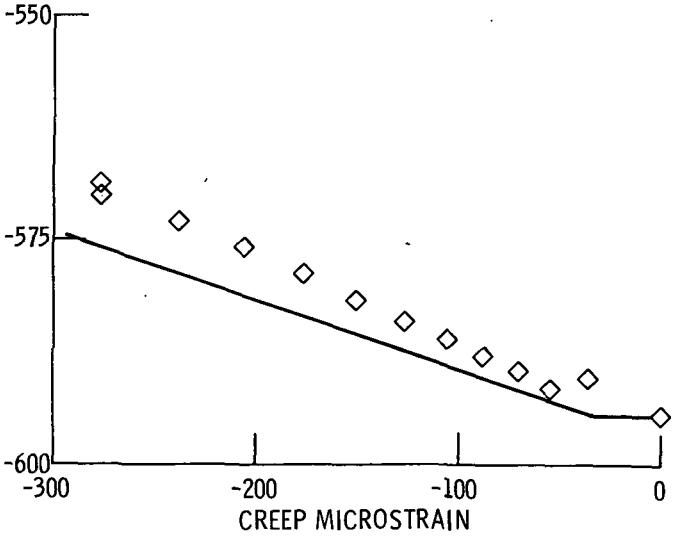

(c) Case 3.

Figure 6. - Comparison of simplified and finite-element creep analyses.

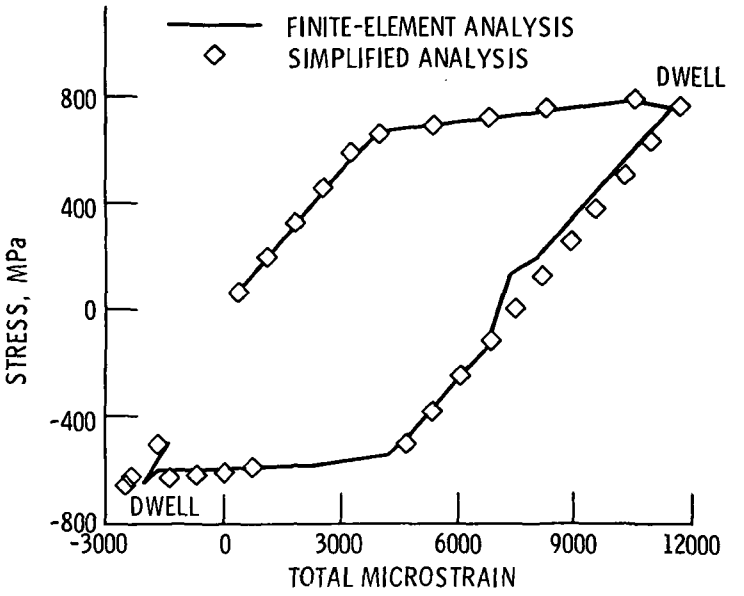

Figure 7. - Comparison of simplified and finite-element cyclic creep analyses for case 4.

1. Report No.	2. Government Accession No.	3. Recipient's Catalog No.
NASA TM-87213		

4. Title and Subtitle	5. Report Date
Cyclic Creep Analysis from Elastic Finite-Element Solutions	6. Performing Organization Code: 533-04-12

7. Author(s)	8. Performing Organization Report No.
A. Kaufman and S.Y. Hwang	E-2872
	10. Work Unit No.

9. Performing Organization Name and Address	11. Contract or Grant No.
National Aeronautics and Space Administration Lewis Research Center Cleveland, Ohio 44135	13. Type of Report and Period Covered: Technical Memorandum

12. Sponsoring Agency Name and Address	14. Sponsoring Agency Code
National Aeronautics and Space Administration Washington, D.C. 20546	

15. Supplementary Notes

A. Kaufman, NASA Lewis Research Center; S.Y. Hwang, South Carolina State College, Orangeburg, South Carolina. Prepared for the 1986 Southeastern Conference on Theoretical and Applied Mechanics, sponsored by the University of South Carolina, Columbia, South Carolina, April 17-18, 1986.

16. Abstract

A uniaxial approach was developed for calculating cyclic creep and stress relaxation at the critical location of a structure subjected to cyclic thermomechanical loading. This approach was incorporated into a simplified analytical procedure for predicting the stress-strain history at a crack initiation site for life prediction purposes. An elastic finite-element solution for the problem was used as input for the simplified procedure. The creep analysis includes a self-adaptive time incrementing scheme. Cumulative creep is the sum of the initial creep, the recovery from stress relaxation and the incremental creep. The simplified analysis was exercised for four cases involving a benchmark notched plate problem. Comparisons were made with elastic-plastic-creep solutions for these cases using the MARC nonlinear finite-element computer code.

17. Key Words (Suggested by Author(s))	18. Distribution Statement
Simplified cyclic analysis; Creep; Structures; Nonlinear analysis	Unclassified - unlimited STAR Category 39

19. Security Classif. (of this report)	20. Security Classif. (of this page)	21. No. of pages	22. Price*
Unclassified	Unclassified		

*For sale by the National Technical Information Service, Springfield, Virginia 22161

National Aeronautics and
Space Administration

Lewis Research Center
Cleveland, Ohio 44135

SECOND CLASS MAIL

ADDRESS CORRECTION REQUESTED

Postage and Fees Paid
National Aeronautics and
Space Administration
NASA-451

Official Business
Penalty for Private Use $300

NASA